

1

On global properties of time-delayed feedback control

Wolfram Just

1.1

Introduction

Topics in control are a genuine subject in engineering and applied mathematics. Such a field was developed in the wake of the second world war [1]. Although it is virtually not possible to give a comprehensive overview of the whole subject it is often an essential feature of standard control approaches to use to some extent structural information about the underlying dynamics, the possibility to reconstruct dynamical equations of motion from measured signal, or focus on simple time independent target states. There exists a rather complete theory for linear systems. Furthermore global aspects of the dynamics can be dealt with by Lyapunov techniques which are applicable when the underlying equations of motion are known. From such a perspective control theory provides a strong link to optimisation problems.

Within control theory different types of methods have been classified. Actually, from the point of view of applications it usually does not matter whether the method is invasive, i.e. a finite control force has to be applied when the target state is reached, or non-invasive. The latter type, often called orbit control in the engineering context, stabilises genuine unstable motion of the dynamical system and requires only small control forces. Such an idea was combined in the early 90th with properties of chaotic dynamical systems to solve the so called pole placement problem for the stabilisation of unstable periodic states by applying tiny control forces [2]. Dynamical systems approaches, i.e. stable and unstable manifolds, were employed to design suitable control algorithms for controlling the huge number of unstable states embedded in chaotic attractors by application of tiny control forces. Although such an idea was known to some extent by engineers it became quite popular among physicists [3].

On the other hand, stabilisation of time-periodic states without any knowledge of the structure of the underlying dynamics still posed some challenge in particular when non-invasive methods are of interest, which can e.g. be used used for spectroscopic purposes as well. Control techniques based on suitable time-delayed feedback of measured signals have been proposed for

Titel. Author(s)

Copyright © 2005 WILEY-VCH Verlag GmbH & Co. KGaA, Weinheim

ISBN: 3-527-XXXXX-X

such a purpose [4] and have been applied to a variety of experimental setups, e.g. for the control of laser systems [5], Taylor-Couette flows [6], in ferromagnetic resonance experiments [7], in electrochemical cells [8], and of course for demonstration purpose in elastomechanics [9] and electronic circuit experiments [10]. Even applications in biosystems have been reported [11], although some of the setups do not result in a completely non-invasive scheme.

Although motion with time-delay results in dynamical systems with infinite-dimensional phase space there exists a fairly comprehensive approach to solve linear equations of motion, in particular for the autonomous case [12]. Thus, most systematic theoretical investigations of time-delayed feedback control have been based so far on linear stability analysis (cf. e.g. [13–15]). Several universal features of the control scheme were uncovered by such an approach. Periodic orbits with an odd number of positive unstable Floquet multipliers cannot be stabilised by plain time-delayed feedback schemes [16], so that such prominent models like the Lorenz equations usually resist time-delayed feedback control. In fact, most examples where time-delayed feedback control has been applied successfully use unstable periodic orbits which were generated in a period doubling cascade where such an “odd number limitation” does not apply. Furthermore, simple time-delayed feedback control fails for systems with fast time scales [17] or systems with large Floquet exponents [18]. Modifications of plain time-delayed feedback control were able to overcome such limitations. Application of an external periodic modulation, so called rhythmic control [19–21], or an unstable control loop [22] can cope with the odd number limitation while the application of multiple time delay, so called extended time-delayed feedback control [17] allows for the stabilisation of periodic states in fast systems. Other important aspects have been addressed as well. Above all methods for the adjustment of suitable delay times have been developed [23–25] and the influence of control loop latency has been analysed in some detail [26,27]. Meanwhile even comprehensive overviews of approaches based on linear analysis are available in the literature (cf. e.g. [28,29]).

Time-delayed feedback control aims at stabilisation of time-periodic states when no information about the underlying dynamical system is available, apart from a measured signal $s(t)$. Thus analytical approaches should be based on general equations of motion which do not make reference to any particular model [14]. Time-delayed feedback control applies a control force $F(t) = K(s(t) - s(t - \tau))$ generated from a time-delayed difference to a dynamical system so that the most general setup reads

$$\dot{\underline{x}}(t) = \underline{f}(\underline{x}(t), F(t)) \quad (1.1)$$

where the measured signal is some, in general unknown, function of the internal degrees of freedom, $s(t) = g(\underline{x}(t))$. If the time delay τ is chosen such that it coincides with an integer multiple of the period of the target state then

the control force will vanish when the target state is reached and the control scheme is potentially non-invasive. Even within such a general setup one is able to discuss the linear stability of the target state and the performance of the control scheme [14]. Results for the stability exponents obtained in such a way are in agreement with measurements (cf. figure 1.1) and yield some of the universal features of time-delayed feedback control. In particular, depending on the control amplitude K a domain, usually an interval, develops where the control signal $s(t) - s(t - \tau)$ tends to zero, all stability exponents develop a negative real part, and control is successful. The boundaries of this interval are the control thresholds. At the lower threshold usually a flip or period doubling bifurcation appears which is responsible for the onset of control. At the upper threshold an instability with nontrivial frequency, i.e. a Hopf bifurcation, occurs. This upper threshold is often less robust and more vulnerable with respect to external perturbations. It is this threshold which will be of interest within our investigations, although similar arguments can be applied to the lower control threshold as well.

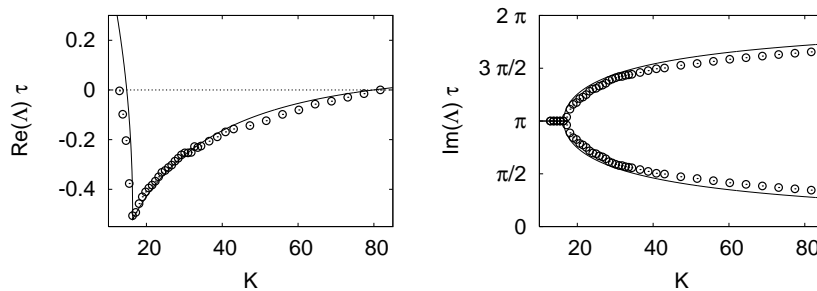


Table 1.1 Typical dependence of the leading Floquet exponent Λ on the control amplitude, for an unstable periodic orbit generated in a period doubling sequence. Symbols: experimental data from an electronic circuit experiment, line: analytical result according to a mean field like expansion (cf. [30] for details).

Since time-delayed feedback control results in a system of differential-difference equations the corresponding linear stability analysis yields infinitely many eigenvalue branches reflecting the infinite-dimensional phase space of the dynamical system. Such branches can be detected even in experiments and may change the simple scenario sketched in figure 1.1 (cf. e.g. [30, 31]). Nevertheless, at a qualitative level one often gets reasonable agreement with the simple theory just sketched.

The basin of attraction, i.e. the set of initial conditions for which control works successfully, is one of the essential objects that cannot be assessed by linear analysis. Such a global feature of the control system is of central interest and has rarely been addressed so far for time-delayed feedback control. If one assumes that the underlying equations of motion are known one would be

able to estimate such basins e.g. by the famous Lyapunov functional method which is available as well for time-delay dynamics (cf. e.g. [32]). Actually, such ideas are very powerful e.g. when one designs numerical tools for root finding. But such a concept cannot be employed easily for time-delayed feedback control. We will discuss such a link in section 1.2. Although global properties of particular model systems subjected to time-delayed feedback control can be estimated by numerical means, e.g. by employing continuation techniques [33] such a strategy can hardly yield generic features of basins of attraction. Furthermore, numerical techniques can be used for the computation of low-dimensional manifolds but are still not able to determine e.g. an infinite-dimensional basin boundary. To overcome such problems basins for time-delayed feedback control have been probed along low-dimensional cross sections by applying well defined perturbations to the system under considerations [34] and the method has been even implemented in experiments [35]. One discovers structures for the basins of attraction that are comparable to those found in low-dimensional dynamical systems. But such features may depend on the underlying equations of motion and do not seem to provide a universal mechanism. On the other hand, a closer look at the instabilities determining the control boundaries can reveal a mechanism for generating basins that just depend on the type of instability and that do not rely on the details of the equations of motion [36]. These ideas will be briefly outlined in section 1.3. The corresponding analytical normal form analysis will be described in section 1.4 and some consequences for time-delayed feedback control will be mentioned. To keep this part less technical we present the analysis within the setup of time-discrete dynamics although similar, but much more involved, considerations can be carried out for the more realistic time-continuous setup as well.

1.2

A comment on control and root finding algorithms

Non-invasive control aims at stabilising unstable orbits of the underlying dynamical system by application of asymptotically small control forces. Thus, in some abstract setting the application of the control loop replaces the original dynamical system by a different one which possesses the former unstable orbit as a stable object. From that point of view such control schemes have something in common with numerical root finding algorithms.

To illustrate the principal aspect of such an idea let us consider for simplicity a time-discrete dynamical system $x_{n+1} = f(x_n)$. An unstable periodic orbit of period p , i.e. a periodic point of order p , $\zeta_* = f^p(\zeta_*)$, should be the desired target state. If the equations of motion are known then the determi-

nation of that object reduces to finding the roots of $f^p(\zeta_*) - \zeta_* = 0$. There are plenty of algorithms available to perform such a task, one of the most famous being the Newton-Raphson method. This method results in an iteration scheme $x_{m+1} = x_m - (f^p(x_m) - x_m)/((f^p)'(x_m) - 1)$ which converges to the periodic point ζ_* for appropriate initial conditions. Thus, the Newton-Raphson method replaces the original dynamics with unstable periodic point ζ_* by a fictitious dynamics with stable point ζ_* . The desired target state can be simply obtained by iteration. In such a sense the scheme could be viewed as a control algorithm. While the Newton-Raphson method has excellent local convergence properties since the sequence converges faster than exponentially towards the target state it is one of the classical examples having often quite poor global properties as the choice of the initial condition is crucial for convergence. The basin of attraction of the target state ζ_* is usually a quite complicated set with fractal basin boundary.

Thus, even for the numerical determination of periodic states one relies on different methods. Again one replaces the original motion by a fictitious dynamics which preserves preferably all periodic points of say period p . Following an idea introduced in [37] which was further refined by [38] and [39] one introduces the differential equation

$$\frac{dx}{ds} = -\gamma(f^p(x) - x) \quad (1.2)$$

such that the stationary states of the solution $x(s)$ yield the desired target states ζ_* . The main benefit of this approach comes from the observation that at least for one-dimensional maps f the global properties of eq.(1.2) can be determined easily as the differential equation (1.2) can be derived from a potential, $dx/ds = -\gamma U'(x)$ where $U(x) = \int (f^p(x) - x) dx$ denotes a Lyapunov function. For such a type of system it is quite easy to show that the energy $U(x(s))$ decreases for $\gamma > 0$ and any solution apart from those which stay at maxima of the potential tends towards a minimum of the potential. The basin of attraction of such a minimum is bounded by the two neighbouring maxima (cf. figure 1.2). Straightforward integration of eq.(1.2) for a few initial conditions yields all the minima of the potential. Reverting the sign of γ interchanges the role of maxima and minima and the same integration procedure now yields the maxima as well. Thus, all critical points of the potential, i.e. all the periodic points of the original dynamical system, can be obtained within a few steps¹. These ideas can be generalised to higher-dimensional maps [37–39] and it is possible to retain to some extent the potential structure

1) The presentation used here differs from the original scheme proposed by Biham and Wenzel which is better adapted for numerical purposes. The approach used here is able to uncover the global properties of the root finding scheme.

which ensures the nice global properties, although it might be more difficult to obtain a priori estimates for the basins of attraction.

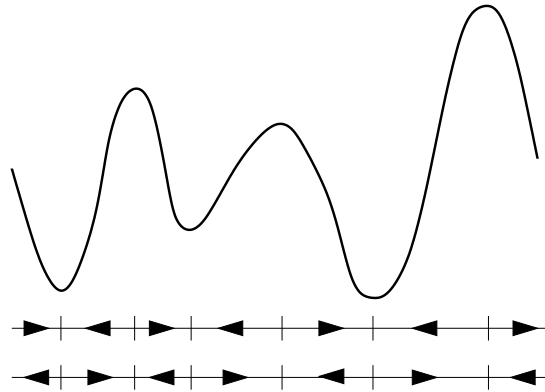


Table 1.2 Diagrammatic view of the potential $U(x) = \int (f^p(x) - x) dx$ governing the dynamics of eq.(1.2). The critical points of the potential and the motion in the one-dimensional phase space for positive and negative values of γ are indicated as well.

There is in fact no need to introduce a time-continuous fictitious dynamics. For instance, one may approximate the derivative by a finite stepsize estimate $(x_{m+1} - x_m)/\Delta s$ and thus obtains the fictitious map

$$x_{m+1} = x_m - \gamma \Delta s (f^p(x_m) - x_m) \quad . \quad (1.3)$$

As long as the stepsize Δs is sufficiently small so that the right hand side is a monotonic function of x_m the good global properties of the time-continuous version are preserved due to the cobweb theorem. There are of course different ways to introduce a time-discrete version and the just mentioned Euler scheme is often not the most efficient way.

A superficial inspection of the scheme (1.3) suggests that a difference involving an iterated state plays a crucial role. From that perspective eq.(1.3) seems to have something in common with time-delayed feedback schemes. Actually, a simple time-delayed feedback scheme for the stabilisation of a period- p orbit reads

$$x_{n+1} = f(x_n) + K(x_n - x_{n-p}) \quad (1.4)$$

and it is tempting to discuss similarities and differences between eqs.(1.3) and (1.4). First of all eq.(1.3) has the same phase space dimension as the original one-dimensional map while the time-delay dynamics (1.4) acts on a p -dimensional phase space. Such an increase of phase space dimension is a characteristic feature of any time-delay system [32]. Thus, already the linear stability properties of both equations are different since the additional degrees of freedom inherent in the time-delay may alter the stability properties

of the target state [30]. It is now not surprising that time-delayed feedback schemes do not share the nice global features of the Biham-Wenzel method since global dynamical features surely depend on the underlying phase space. Time-delayed feedback schemes, like eq.(1.4), have of course the advantage to be based on the real time dynamics so that an implementation in real applications is possible. It would be tempting to improve time-delayed feedback control in such a way that it shares the nice potential properties of root finding algorithms, but no such improvement seems to be available at the moment. The study of global features of time-delayed feedback control is nevertheless of great interest and nice global features like for the Biham-Wenzel scheme are surely the desired goal. Above all, a generic mechanism is needed which is independent of the underlying model, like the potential dynamics in the case of the Biham-Wenzel method, to determine the basins of attraction and the global performance of time-delayed feedback schemes.

1.3

Codimension-two bifurcations and basins of attraction

Determination of basins of attraction is already a challenge for nonlinear ordinary differential equations and one cannot expect to give a full account for time-delay dynamics. Here we will identify a simple mechanism based on local bifurcation theory which determines some basin of attraction in a generic way and which proves its relevance for time-delayed feedback schemes.

1.3.1

The transition from super- to subcritical behaviour

Let us just recall a few elementary features of Hopf bifurcations although such facts can be found in graduate textbooks (cf. e.g. [40]). When a system experiences a Hopf bifurcation an instability takes place where a fixed point becomes unstable with respect to two oscillating modes². Thus the motion can be reduced to a two-dimensional coordinate, usually a complex number $z(t)$, which obeys the so call normal form

$$\dot{z}(t) = \lambda z(t) + rz(t)|z(t)|^2 \quad . \quad (1.5)$$

² Strictly speaking a Hopf bifurcation denotes an instability of a fixed point in a time-continuous system. Later on we will apply such a concept to the instability of periodic orbits as well, i.e. to fixed points in time-discrete maps. In such a case one calls an instability caused by a complex conjugated pair of eigenvalues often a Neimark-Sacker bifurcation since some additional strong resonance conditions become important (cf. appendix 1.A). Here, in order to simplify the notation, we are a little bit sloppy with the notation and call such an instability a Hopf bifurcation as well.

Derivation of such an effective equation of motion can be found in textbooks (cf. section 1.4.1 as well). The coefficient of the linear part coincides with the critical eigenvalue. $\text{Re}(\lambda) < 0$ yields a stable fixed point $z = 0$, a case which we will call the subthreshold regime, while $\text{Re}(\lambda) > 0$ yields an unstable fixed point, the superthreshold regime. The cubic coefficient r is essential for the nontrivial dynamics in the vicinity of the instability. Actually, from the very beginning one can confine to real valued coefficients. Introducing polar coordinates $z = \rho \exp(i\phi)$ eq.(1.5) is written as

$$\dot{\rho}(t) = \text{Re}(\lambda)\rho(t) + \text{Re}(r)\rho^3(t) \quad (1.6a)$$

$$\dot{\phi}(t) = \text{Im}(\lambda) + \text{Im}(r)\rho^2(t) \quad (1.6b)$$

so that imaginary parts of the coefficients just cause an amplitude dependent oscillation. Equation (1.6a) obviously has a nontrivial stationary solution $\rho_\ell = (-\text{Re}(\lambda)/\text{Re}(r))^{1/2}$ whenever the square root is real valued. This nontrivial solution corresponds to a limit cycle of radius ρ_ℓ . Thus, if $\text{Re}(r) < 0$ the limit cycle exists for $\text{Re}(\lambda) > 0$, i.e. in the superthreshold regime where the trivial fixed point is unstable, while for $\text{Re}(r) > 0$ the nontrivial solution exists in the region $\text{Re}(\lambda) < 0$, i.e. the subthreshold regime (cf. figure 1.3). The stability of the resulting limit cycle can be easily evaluated from eq.(1.6a) by computing the derivative of the right hand side at ρ_ℓ , $-2\text{Re}(\lambda)$. The limit cycle is stable for $\text{Re}(r) < 0$, the so called supercritical case, and unstable for $\text{Re}(r) > 0$, the subcritical case³. The features are summarised in figure 1.3.



Table 1.3 Diagrammatic view of a supercritical (left: $\text{Re}(r) < 0$) and subcritical (right: $\text{Re}(r) > 0$) Hopf bifurcation (cf. eq.(1.5)). Full line: stable fixed point/limit cycle, broken line: unstable fixed point/limit cycle. Bifurcation parameter $\text{Re}\lambda$ increases from left to right.

While a supercritical transition is continuous when changing the bifurcation parameter the subcritical transition is discontinuous showing hysteresis as well since a different dynamical state is attained in the superthreshold regime. In addition, in the subthreshold regime the unstable limit cycle which surrounds the stable fixed point yields the basin boundary (cf. figure 1.4). Thus subcritical behaviour always suffers from small basins since the coexisting unstable limit cycle contracts towards the fixed point when the bifurcation point is approached. No such feature exists for the supercritical transition where the

³ Alternative notions for super-/subcritical bifurcations that can be found in the literature are continuous/discontinuous transitions or forward/inverse bifurcation.

basin is determined by some global feature of the dynamics. Thus basins remain large even close to the bifurcation point. This generic mechanism works in higher-dimensional phase spaces as well where the stable manifold of the unstable limit cycle yields the basin boundary. Locally the basin has the topology of a higher-dimensional cylinder (cf. figure 1.4).

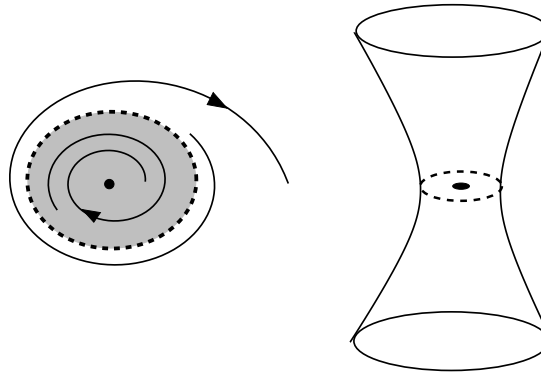


Table 1.4 Left: diagrammatic view of the two-dimensional phase space portrait close to a subcritical Hopf bifurcation in the subthreshold regime: unstable limit cycle (broken line) and basin of the stable fixed point (shaded). Right: geometry of the stable manifold of the unstable limit cycle (broken line), i.e. the basin boundary of the stable fixed point, in a three-dimensional phase space.

When $\text{Re}(\lambda)$ changes sign a Hopf bifurcation takes place which is either super- or subcritical depending on the sign of $\text{Re}(r)$. If the latter quantity becomes small and changes sign as well then a codimension-two bifurcation takes place since two conditions $\text{Re}(\lambda) = 0$ and $\text{Re}(r) = 0$ have to be satisfied. Such an higher-order instability governs the transition from super- to subcritical behaviour. The universal features of such a transition depend on higher order terms in the normal form (1.5) and yield some information about the limit cycles involved in the Hopf bifurcation and the occurring hysteresis (cf. e.g. [40] for further details).

1.3.2

Probing basins of attraction in experiments

As shown in the previous section subcritical bifurcations, i.e. discontinuous transitions and hysteresis, yield a limitation for the basin of the stable state at least when the bifurcation point is approached. This generic mechanism can also be relevant for time-delayed feedback control, e.g. at the upper control threshold when a subcritical Hopf bifurcation occurs. The principal aspects of such a mechanism can be demonstrated by numerical simulations (cf. section 1.4.2 or [36]) and it even proves its relevance in real experiments [35]. Here we

just summarise the essential features. More details about the experiment can be found in a later chapter of the book.

Detection of discontinuous transitions e.g. at the upper control threshold, the corresponding bistability, and recording hysteresis is easily accomplished by an adiabatic increase respectively decrease of the control amplitude. Discontinuity in the amplitude of the control signal $s(t) - s(t - \tau)$ shows up (cf. figure 1.5 for an experimental realisation in an electronic circuit experiment). Thus, subcritical transitions are easily detected. Probing the basin of attraction of the stabilised periodic orbit in the subthreshold regime is a much more challenging task. The phase space of differential-difference equations is infinite-dimensional since the whole history enters the dynamics. The basin and the basin boundary are infinite-dimensional objects as well as. Nevertheless, close to the bifurcation point the basin admits the geometry sketched in figure 1.4. Thus, if one applies a well defined perturbation to the controlled system, e.g. a voltage pulse at a definite value of the phase of the periodic orbit, then one probes the basin along a low-dimensional cross section in phase space, e.g. along a line or a two-dimensional surface. By monitoring the maximal strength of the pulse such that the system returns to the stabilised state one obtains an estimate for the diameter of the basin of attraction in this cross section. Experimental data displayed in figure 1.5 show indeed the characteristic S-shape for the diameter of the basin (cf. figure 1.3) when recorded in dependence on the control amplitude. Thus, subcritical bifurcations yield reduced basins of attraction and an enhanced sensitivity of the controlled systems with respect to external perturbations.

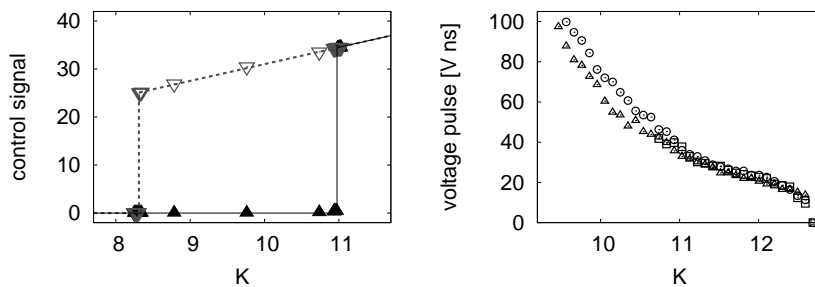


Table 1.5 Left: dependence of the amplitude of the control signal on the control amplitude K in an electronic circuit experiment: adiabatic increase (black, full symbols, line), adiabatic decrease (grey, open symbols, broken line) of K . Lines are a guide for the eye. Right: critical voltage pulse to destroy the controlled state, in dependence on the control amplitude. Different symbols correspond to different durations of the pulse.

1.4

A case study of global features for time-delayed feedback control

Determination of the type of instability which limits control domains for time-delayed feedback control is in principle quite straightforward [36]. But explicit computations of such normal forms become quite involved for time-continuous time-delay equations [32] even when fairly simple model systems are considered (cf. e.g. [41, 42]). Here we want to illustrate the relevance of sub- and supercritical transitions for the formation of basins of attraction. For the purpose of visualisation we even want to avoid the problems that are related with infinite-dimensional phase spaces. Since we are interested in the principal mechanism we focus on the simplest setup, namely the stabilisation of fixed points in a one-dimensional map. In view of the previous remarks it is obvious that for such models there exist much more powerful tools for controlling unstable fixed points. But the case study presented here gives some insight into global features of time-delayed feedback control and the results can be generalised to time-continuous systems as well. Moreover, the analysis presented here for the time-discrete setup is simpler from the technical point of view, although it has only relevance for real control experiments at a qualitative level.

1.4.1

Analytical bifurcation analysis of one-dimensional maps

Let us consider a one-dimensional map $x_{n+1} = f(x_n)$ with fixed point $\tilde{\zeta}_* = f(\tilde{\zeta}_*)$. To stabilise the fixed point a simple time-delayed feedback scheme is applied

$$x_{n+1} = f(x_n) + K(x_n - x_{n-1}) \quad . \quad (1.7)$$

Actually, the phase space dimension of eq.(1.7) has increased just by one and it is for that reason why the analysis of this time-delay system stays to be rather straightforward. In a neighbourhood of the fixed point a Taylor series expansion of eq.(1.7) up to third order yields, using the variable $\delta x_n = x_n - \tilde{\zeta}_*$

$$\delta x_{n+1} = f'(\tilde{\zeta}_*)\delta x_n + K(\delta x_n - \delta x_{n-1}) + \frac{f''(\tilde{\zeta}_*)}{2}(\delta x_n)^2 + \frac{f'''(\tilde{\zeta}_*)}{3!}(\delta x_n)^3 + \dots \quad . \quad (1.8)$$

It is now the scope to transform such an equation of motion into the normal form (cf. eq.(1.31)). Details of the formal calculation are summarised in appendix 1.A.

Using the state vector $\underline{y}_n = (y_n^{(1)}, y_n^{(2)}) = (\delta x_n, \delta x_{n-1})$ eq.(1.8) can be cast into a nonlinear two-dimensional map (cf. eq.(1.28)). The linear part of the

motion is governed by the two-dimensional matrix

$$\underline{\underline{A}} = \begin{pmatrix} f'(\xi_*) + K & -K \\ 1 & 0 \end{pmatrix} . \quad (1.9)$$

Stability of the trivial solution is easily expressed in terms of the determinant and the trace of this matrix. Here we are interested in cases where we are close to a Hopf bifurcation, i.e. usually close to the upper control threshold. Then the matrix (1.9) admits a complex conjugated pair of eigenvalues μ_c, μ_c^* with modulus one, $\mu_c = \exp(i\varphi_c)$. Thus

$$1 = \det(\underline{\underline{A}}) = K_c \quad (1.10)$$

and

$$\text{tr}(\underline{\underline{A}}) = f'(\xi_*) + K_c = \mu_c + \mu_c^* = 2 \cos(\varphi_c) \in (-2, 2) . \quad (1.11)$$

The eigenvector for the eigenvalue μ_c is obviously given by

$$\underline{u}_c = \begin{pmatrix} \mu_c \\ 1 \end{pmatrix} \quad (1.12)$$

while the eigenvector of the corresponding adjoint eigenvalue problem (cf. eq.(1.29b)) reads

$$\underline{v}_c^\dagger = (-\mu_c, 1) . \quad (1.13)$$

If the control amplitude K deviates from its critical value $K_c = 1$ then the linear part changes by the amount

$$\underline{\underline{\delta A}} = \delta K \begin{pmatrix} 1 & -1 \\ 0 & 0 \end{pmatrix} \quad (1.14)$$

when $\delta K = K - K_c$ denotes the distance of the control amplitude from the control boundary.

So far we have written down the linear terms of the equations of motion (1.8). In order to determine the normal form we have to consider quadratic and cubic nonlinearities as well. Using the notation introduced in appendix 1.A the quadratic and cubic terms can be expressed through bilinear and trilinear expressions, $B : \underline{y}_n : \underline{y}_n :$ and $C : \underline{y}_n : \underline{y}_n : \underline{y}_n :$ respectively, where

$$B : \underline{u} : \underline{v} : = \frac{f''(\xi_*)}{2} \begin{pmatrix} u^{(1)}v^{(1)} \\ 0 \end{pmatrix} \quad (1.15a)$$

$$C : \underline{u} : \underline{v} : \underline{w} : = \frac{f'''(\xi_*)}{3!} \begin{pmatrix} u^{(1)}v^{(1)}w^{(1)} \\ 0 \end{pmatrix} . \quad (1.15b)$$

The evolution equation (1.8) has been cast into the vector notation of eq.(1.28) and for the coefficients of the normal form (1.31) the expressions (1.37) and (1.39) can be evaluated readily.

For the unfolding parameter (1.37) we obtain, using eqs.(1.12), (1.13), and (1.14)

$$\varepsilon = \frac{\langle \underline{v}_c | \underline{\delta A} \underline{u}_c \rangle}{\langle \underline{v}_c | \underline{u}_c \rangle} = \delta K \frac{\mu_c(1 - \mu_c)}{1 - \mu_c^2} = \mu_c \frac{\delta K \exp(-i\varphi_c/2)}{2 \cos(\varphi_c/2)} \quad (1.16)$$

where we have used the polar representation of the critical eigenvalue as well, $\mu_c = \exp(i\varphi_c)$. Since

$$\operatorname{Re}(\varepsilon/\mu_c) = \delta K/2 \quad (1.17)$$

the trivial fixed point is stable if $\delta K < 0$, i.e. below the control threshold while control fails above that threshold, $\delta K > 0$ (cf. appendix 1.B for the linear stability criterion).

The nature of the Hopf bifurcation is determined by the cubic coefficient (1.39). The two auxiliary vectors (1.35) are just computed from eqs.(1.9), (1.10), (1.12), and (1.15a)

$$\begin{aligned} \underline{\alpha} &= \frac{f''(\xi_*)}{2} \frac{1}{\det(\mu_c^2 \underline{1} - \underline{A})} \begin{pmatrix} \mu_c^2 & -1 \\ 1 & \mu_c^2 - f'(\xi_*) - 1 \end{pmatrix} \begin{pmatrix} \mu_c^2 \\ 0 \end{pmatrix} \\ &= \frac{f''(\xi_*)/2}{(\mu_c^2 - \mu_c)(\mu_c^2 - 1/\mu_c)} \begin{pmatrix} \mu_c^4 \\ \mu_c^2 \end{pmatrix} \end{aligned} \quad (1.18a)$$

$$\begin{aligned} \underline{\beta} &= \frac{f''(\xi_*)}{2} \frac{1}{\det(\underline{1} - \underline{A})} \begin{pmatrix} 1 & -1 \\ 1 & -f'(\xi_*) \end{pmatrix} \begin{pmatrix} |\mu_c|^2 \\ 0 \end{pmatrix} \\ &= \frac{f''(\xi_*)/2}{(1 - \mu_c)(1 - 1/\mu_c)} \begin{pmatrix} 1 \\ 1 \end{pmatrix}. \end{aligned} \quad (1.18b)$$

Now the evaluation of the terms entering the coefficient (1.39) is straightforward, applying the definitions (1.15)

$$\begin{aligned} \frac{\langle \underline{v}_c | B : \underline{u}_c^* : \underline{\alpha} : \rangle}{\langle \underline{v}_c | \underline{u}_c \rangle} &= - \left(\frac{f''(\xi_*)}{2} \right)^2 \frac{\mu_c^4}{(1 - \mu_c^2)(\mu_c^2 - \mu_c)(\mu_c^2 - 1/\mu_c)} \\ &= \mu_c \left(\frac{f''(\xi_*)}{2} \right)^2 \frac{i}{8 \sin \varphi_c \sin(\varphi_c/2) \sin(3\varphi_c/2)} \end{aligned} \quad (1.19a)$$

$$\begin{aligned} \frac{\langle \underline{v}_c | B : \underline{u}_c : \underline{\beta} : \rangle}{\langle \underline{v}_c | \underline{u}_c \rangle} &= - \left(\frac{f''(\xi_*)}{2} \right)^2 \frac{\mu_c^2}{(1 - \mu_c^2)(1 - \mu_c)(1 - 1/\mu_c)} \\ &= \mu_c \left(\frac{f''(\xi_*)}{2} \right)^2 \frac{-i}{8 \sin \varphi_c \sin^2(\varphi_c/2)} \end{aligned} \quad (1.19b)$$

$$\begin{aligned} \frac{\langle \underline{v}_c | C : \underline{u}_c : \underline{u}_c : \underline{u}_c^* : \rangle}{\langle \underline{v}_c | \underline{u}_c \rangle} &= - \left(\frac{f'''(\xi_*)}{3!} \right) \frac{\mu_c^2}{1 - \mu_c^2} \\ &= \mu_c \left(\frac{f'''(\xi_*)}{3!} \right) \frac{-i}{2 \sin(\varphi_c)}. \end{aligned} \quad (1.19c)$$

Thus

$$\operatorname{Re}(r/\mu_c) = 0 \quad (1.20)$$

since all contributions to the cubic coefficient are imaginary⁴. Hence the control law (1.7) just realises the transition between sub- and supercritical behaviour (cf. appendix 1.B for the conditions on super- and subcritical Hopf bifurcations for maps), no matter what the values of the second and third derivatives are, i.e. no matter what kind of one-dimensional map is considered. The result is in fact far from surprising since it is due to some hidden symmetry which is shared by the control law (1.7). If one considers the value of the critical coupling $K_c = 1$ then the Jacobian of the corresponding two-dimensional map is easily computed to be (cf. eq.(1.9))

$$\text{Jac}_f(\underline{x}) = \begin{pmatrix} f'(x^{(1)}) + K_c & -K_c \\ 1 & 0 \end{pmatrix}. \quad (1.21)$$

The determinant of the Jacobian equals one and the two-dimensional map is area preserving. Hence, all the dissipative contributions to the normal form, i.e. the real parts of the coefficients, will vanish. This particular symmetry will be destroyed if a different type of coupling is considered, and a transition from sub- to supercritical behaviour can be realised.

1.4.2

Dependence of sub- and supercritical behaviour on the observable

The control scheme (1.7) can be modified in a simple way by altering the observable from which the time-delayed control force is derived. If we keep for simplicity the additive coupling of the control force then the dynamics is determined by

$$x_{n+1} = f(x_n) + K(g(x_n) - g(x_{n-1})) \quad (1.22)$$

where $g(x_n)$ denotes the measured signal which depends on the state x_n in general in a nonlinear way. With a suitable choice of the observable $g(x_n)$ it is possible to generate supercritical behaviour at the upper control threshold. It is rather straightforward to apply the analytical perturbation scheme of the previous section to the current setup. But here we just illustrate the essential behaviour in a phenomenological way by a simple numerical simulation.

For that purpose let us choose $g(x) = x + \lambda x^2$. The free parameter λ allows for tuning the nonlinearity of the measured signal. The choice $\lambda = 0$ corresponds to the setup of the previous section with degenerated bifurcations at the upper control threshold. For the underlying dynamical system we employ the logistic map $f(x) = 1 - ax^2$ at parameter value $a = 1.6$ to ensure for chaotic motion. The control thresholds can be easily computed using linear stability analysis. Actually, comparing eq.(1.7) with eq.(1.22) it is obvious that the previous results can be used when K is replaced by $g'(\xi_*)K$. In particular,

4) The imaginary part diverges if $\varphi_c = 0, \pm\pi, \pm 2\pi/3$, i.e. in the case of a strong resonance.

the upper control threshold is given by $g'(\xi_*)K_c = 1$. For a sensible comparison of results for different observables it is therefore appropriate to use the normalised control amplitude $g'(\xi_*)K$ since this quantity governs the linear stability properties.

Numerical simulations show that a supercritical Hopf bifurcation is found for $\lambda > 0$ while for $\lambda < 0$ subcritical behaviour prevails (cf. figure 1.6). The supercritical transition is continuous and no hysteresis or bistability occurs when one compares results obtained from an adiabatic increase and decrease of the control amplitude. The subcritical transition for $\lambda < 0$ is discontinuous. Actually, phase space points escape to infinity in the superthreshold regime as a result of a lack of phase space contraction and dissipation in the model (cf. previous section).

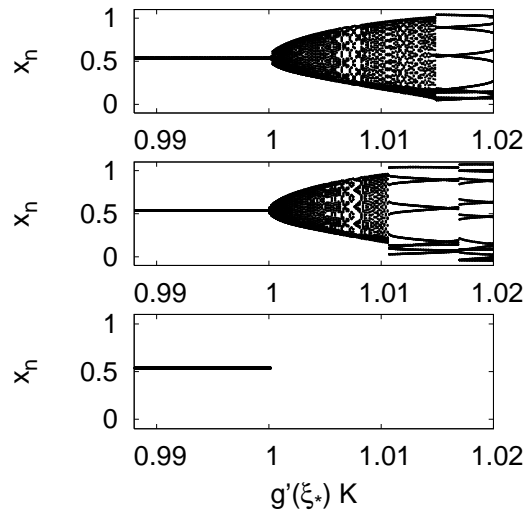


Table 1.6 Bifurcation diagrams of the model (1.22) with $f(x) = 1 - ax^2$, $g(x) = x + \lambda x^2$, and $a = 1.6$. Top: $\lambda = 0.2$ adiabatic increase of the control amplitude, middle: $\lambda = 0.2$ adiabatic decrease of the control amplitude, bottom: $\lambda = -0.2$ adiabatic increase of the control amplitude. Successful control for $g'(\xi_*)K < 1$. Continuous transition for $\lambda = 0.2$ with regions of additional bistability above the control threshold. Discontinuous transition for $\lambda = -0.2$ where the solution escapes to infinity for $K > K_c$.

The transition from super- to subcritical behaviour which has been induced by the change of observable is accompanied by a corresponding change in the global dynamical features. Figure 1.7 shows the basins of attraction of the stabilised fixed point in the subthreshold regime, $K < K_c$, for positive and negative values of λ , i.e. for the super- and subcritical Hopf bifurcation, respectively. In the subcritical case, $\lambda < 0$, the basin of attraction is restricted to a small neighbourhood of the target state, in particular when the control amplitude is close to the critical value K_c . No such constraint is observed in

the supercritical case, $\lambda > 0$, where the basin of attraction remains large even when the boundary of the control interval is approached. Thus, the suitable choice of observable has a profound effect on the global properties of the control, as predicted by the previous analytical considerations.

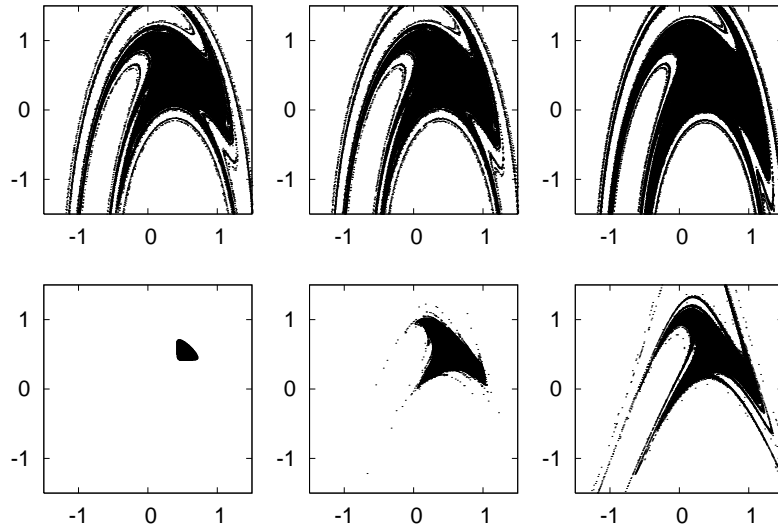


Table 1.7 Basin of attraction of the model (1.22) for supercritical (top: $\lambda = 0.2$) and subcritical (bottom: $\lambda = -0.2$) transitions, displayed in the x_0 - x_{-1} plane of initial conditions and different values of the control amplitude: $g'(\zeta_*)K = 0.999$ (left), 0.99 (middle), 0.95 (right). Black dots mark initial conditions resulting in successful stabilisation of the target state $\zeta_* = 0.537\dots$. Basins are essentially independent of K in the supercritical case while a considerable reduction of the basin in the subcritical case occurs close to the control threshold.

1.4.3

Influence of the coupling of the control force

As long as the desired unstable target state is embedded in a chaotic attractor one may improve the control performance by applying the control force only if the actual state is close to the target state. Such events happen because of the recurrence properties of chaotic motion. Within the context of time-delayed feedback control such events can be identified easily since the control force becomes small when the system is close to the target state. Corresponding ideas have been proposed for time-delayed feedback control from the very beginning [4]. Within the context of the previous example it means that one caps the control force $x_n - x_{n-1}$ when its value becomes too large. In terms of a mathematical model that means

$$x_{n+1} = f(x_n) + Kh(x_n - x_{n-1}) \quad (1.23)$$

where the coupling function $h(x)$ is odd, $h(x) = h(-x)$, has slope one for small argument to keep the results comparable to the previous investigations, $h'(0) = 1$, and saturates or decays for large values of the argument. Indeed such a coupling function will enhance the control performance since it is able to induce supercritical Hopf bifurcations at the upper control threshold and thus enlarges basins of attraction even without chaotic recurrence to the target state.

It is quite straightforward to supply the details of the analytical perturbation expansion when we assume $h'(0) = 1$ and $h''(0) = 0$. Recall that with these assumptions the Taylor series expansion reads

$$h(x_n - x_{n-1}) = x_n - x_{n-1} + \frac{h'''(0)}{3!}(x_n - x_{n-1})^3 + \dots \quad (1.24)$$

It is obvious that the analysis of section 1.4.1 still applies as far as linear and quadratic terms are concerned (cf. eq.(1.8)). Just the cubic nonlinearity (cf. eq.(1.15b)) changes since in view of eq.(1.24) and $K_c = 1$ an additional additive contribution occurs

$$C : \underline{u} : \underline{v} : \underline{w} : = \frac{f'''(\xi_*)}{3!} \begin{pmatrix} u^{(1)}v^{(1)}w^{(1)} \\ 0 \end{pmatrix} + \frac{h'''(0)}{3!} \begin{pmatrix} (u^{(1)} - u^{(2)})(v^{(1)} - v^{(2)})(w^{(1)} - w^{(2)}) \\ 0 \end{pmatrix} \quad (1.25)$$

Thus, for the computation of the cubic coefficient of the normal form we just have to recalculate eq.(1.19c) which is pretty straightforward using the eigenvector (1.12) and (1.13)

$$\begin{aligned} & \frac{\langle \underline{v}_c | C : \underline{u}_c : \underline{u}_c : \underline{u}_c^* : \rangle}{\langle \underline{v}_c | \underline{u}_c \rangle} \\ &= - \left(\frac{f'''(\xi_*)}{3!} \right) \frac{\mu_c^2}{1 - \mu_c^2} - \frac{h'''(0)}{3!} \frac{\mu_c(\mu_c - 1)(\mu_c - 1)(\mu_c^* - 1)}{1 - \mu_c^2} \\ &= \mu_c \left(\frac{f'''(\xi_*)}{3!} \right) \frac{-i}{2 \sin(\varphi_c)} + \mu_c \frac{h'''(0)}{3!} \frac{2 \exp(-i\varphi_c/2) \sin^2(\varphi_c/2)}{\cos(\varphi_c/2)} \quad (1.26) \end{aligned}$$

Now eqs.(1.19a), (1.19b), and (1.26) yield

$$\text{Re}(r/\mu_c) = \frac{2h'''(0)}{3!} \sin^2(\varphi_c/2) \quad (1.27)$$

Supercritical behaviour occurs if $h'''(0) < 0$ which corresponds locally to a saturation of the control force, while subcritical behaviour and corresponding deterioration of the basins is caused for $h'''(0) > 0$. The local codimension-two analysis thus nicely complies with the observations described above and highlights the importance of the coupling scheme for global properties of time-delayed feedback control.

1.5

Conclusion

Time-delayed feedback control has been developed to stabilise time-periodic states with tiny control forces when no detailed information about the underlying dynamics is available. Meanwhile properties of such control schemes are quite well understood as far as linear stability is concerned. But even from the linear perspective there are unsolved problems of experimental relevance. Apart from very preliminary numerical studies of model systems (cf. e.g. [13,31]) it is rather unclear how properties of the measured signal and the coupling of the control force to the internal degrees of freedom affect the control properties in detail. While such questions are addressed by standard control theory in great detail, comparable results are still missing for time-delayed feedback control.

Apart from numerical simulations of model systems properties of time-delayed feedback control are scarcely investigated beyond linear stability analysis. For instance, almost no analytical results are available concerning basins of attraction or the robustness of the control scheme with respect to external, e.g. stochastic, perturbations. While such results are delivered by standard control theory using Lyapunov functions such a strategy cannot be applied directly to time-delayed feedback schemes unless the structure of the underlying equations of motion is known. In the near future one may hope that the application of numerical continuation schemes to particular models of time-delayed feedback control may give some insight into global properties of the delay dynamics, c.f. e.g. [43]. The ultimate goal, however, should be a modification of time-delayed feedback schemes such that generic systems show good Lyapunov stability properties.

The case study presented here followed a different less ambitious route. Application of bifurcation theory to time-delay dynamics may give some insight into generic features of time-delayed feedback control. The analysis of local higher-order codimension bifurcations related with the behaviour at control thresholds is able to yield information about the global phase space structure. The analysis presented here for the time-discrete case can be performed in the more realistic time-continuous setup as well [36]. Such approaches are potentially able to yield universal global features of time-delayed feedback control as demonstrated in the previous section. It is furthermore tempting to apply such ideas for analysing the influence of external perturbations beyond the linear response regime, to employ global phase space structures for implementing targeting procedures (cf. e.g. [3]) for time-delayed feedback control, and to study the interrelation between spatial degrees of freedom and time delay. Thus, there are still plenty of interesting problems around which are of general interest for time-delay dynamics and which are not restricted to the study of control problems.

Acknowledgement

The concepts which have been addressed in this chapter were developed in collaboration with many colleagues. In particular, I would like to thank A. Amann, N. Baba, H. Benner, T. Bernard, D. Gauthier, J. Hołyst, P. Hövel, N. B. Janson, K. Kacperski, H. Kantz, B. Krauskopf, K. Pyragas, E. Reibold, E. Schöll, and J. E. S. Socolar.

1.A

Normal form reduction

Normal form calculations for Hopf bifurcations are a standard procedure. To keep the presentation self-contained and since appropriate closed expressions for the normal form parameters are rarely available in the literature we here just recall the computation. Suppose a system with trivial fixed point $\underline{y} = 0$ experiences a Hopf bifurcation. Close to the critical point a Taylor series expansion of the d -dimensional map yields the expression

$$\underline{y}_{n+1} = \underline{A} \underline{y}_n + \underline{\delta A} \underline{y}_n + B : \underline{y}_n : \underline{y}_n : + C : \underline{y}_n : \underline{y}_n : \underline{y}_n : + \dots \quad (1.28)$$

The matrix \underline{A} governs the linear part of the motion at the bifurcation point. Thus the corresponding eigenvalue problem

$$\underline{A} \underline{u}_c = \mu_c \underline{u}_c \quad (1.29a)$$

$$\underline{v}_c^\dagger \underline{A} = \mu_c \underline{v}_c^\dagger \quad (1.29b)$$

possesses a complex conjugated pair of eigenvalues μ_c, μ_c^* , where $|\mu_c| = 1$. Eq.(1.29b) just states the adjoint eigenvalue equation with \underline{v}_c^\dagger denoting the Hermitian conjugate. Such an eigenvector will turn out to be quite useful for analytical calculations. The additional linear contribution to eq.(1.28), $\underline{\delta A}$, is supposed to be small and takes the deviation from the bifurcation point into account. Furthermore, nonlinear quadratic and cubic contributions to the equations of motion are captured by the tensors B and C^5 .

We are looking for a two-dimensional surface in the full phase space which is invariant with respect to the dynamics of eq.(1.28), which is tangent to the plane spanned by the two critical vectors \underline{u}_c and \underline{u}_c^* when a system at the bifurcation point is considered, and which thus captures the slow part of motion in the vicinity of the critical point. Such a manifold can be written in terms of

5) The ν -component of $B : \underline{u} : \underline{v} :$ is given by $\sum_{\mu\rho} B^{(\nu\mu\rho)} u^{(\mu)} v^{(\rho)}$. In view of eq.(1.28) we assume a symmetric expression $B : \underline{u} : \underline{v} := B : \underline{v} : \underline{u} :$ and employ homogeneity $B : \alpha \underline{u} : \underline{v} := \alpha B : \underline{u} : \underline{v} :$ and additivity $B : \underline{u} + \underline{w} : \underline{v} := B : \underline{u} : \underline{v} : + B : \underline{w} : \underline{v} :$. An analogous notation is used for the cubic nonlinearity $C : \underline{u} : \underline{v} : \underline{w} :$.

a complex valued coordinate z_n as

$$\underline{y}_n = \underline{u}_c z_n + \underline{u}_c^* z_n^* + \underline{\delta} z_n + \underline{\delta}^* z_n^* + \underline{\alpha} z_n^2 + \underline{\alpha}^* (z_n^*)^2 + 2\underline{\beta} |z_n|^2 + \underline{\gamma} z_n |z_n|^2 + \dots \quad (1.30)$$

Here \dots denotes the remaining cubic nonresonant contributions and terms of higher order. The additional linear term $\underline{\delta} z_n$ accounts for deviations from the bifurcation point and is therefore of the same small order as $\underline{\delta A}$. It is our goal to fix the parameters $\underline{\alpha}$, $\underline{\beta}$, $\underline{\gamma}$, and $\underline{\delta}$ in such a way that the dynamics for the slow coordinate z_n obeys the so called normal form

$$z_{n+1} = (\mu_c + \varepsilon) z_n + r z_n |z_n|^2 + \dots \quad (1.31)$$

where the small deviation from the critical point, ε , is assumed to be of the order $\mathcal{O}(z^2)$.

Employing the invariance of the surface (1.30) we can immediately obtain explicit expressions for the coefficients appearing in eq.(1.31). On the one hand eq.(1.30) yields

$$\begin{aligned} \underline{y}_{n+1} &= \underline{u}_c z_{n+1} + \underline{u}_c^* z_{n+1}^* + \underline{\delta} z_{n+1} + \underline{\delta}^* z_{n+1}^* \\ &\quad + \underline{\alpha} z_{n+1}^2 + \underline{\alpha}^* (z_{n+1}^*)^2 + 2\underline{\beta} |z_{n+1}|^2 + \underline{\gamma} z_{n+1} |z_{n+1}|^2 + \dots \\ &= \left(\mu_c z_n + \varepsilon z_n + r z_n |z_n|^2 + \dots \right) \underline{u}_c + \left(\mu_c^* z_n^* + \varepsilon^* z_n^* + r^* z_n^* |z_n|^2 + \dots \right) \underline{u}_c^* \\ &\quad + \mu_c \underline{\delta} z_n + \mu_c \underline{\delta}^* z_n^* + \mu_c^2 \underline{\alpha} z_n^2 + (\mu_c^*)^2 \underline{\alpha}^* (z_n^*)^2 + 2\underline{\beta} |z_n|^2 + \mu_c \underline{\gamma} z_n |z_n|^2 \end{aligned} \quad (1.32)$$

where for the last step eq.(1.31) has been employed. On the other hand the same quantity is, according to eq.(1.28), given by

$$\begin{aligned} \underline{y}_{n+1} &= \underline{A} \underline{y}_n + \underline{\delta A} \underline{y}_n + B : \underline{y}_n : \underline{y}_n : + C : \underline{y}_n : \underline{y}_n : \underline{y}_n : + \dots \\ &= \underline{A} \underline{u}_c z_n + \underline{A} \underline{u}_c^* z_n^* + \underline{A} \underline{\alpha} z_n^2 + \underline{A} \underline{\alpha}^* (z_n^*)^2 + 2\underline{A} \underline{\beta} |z_n|^2 + \underline{A} \underline{\gamma} z_n |z_n|^2 \\ &\quad + \underline{A} \underline{\delta} z_n + \underline{A} \underline{\delta}^* z_n^* + \underline{\delta A} \underline{u}_c z_n + \underline{\delta A} \underline{u}_c^* z_n^* \\ &\quad + B : \underline{u}_c : \underline{u}_c : z_n^2 + B : \underline{u}_c^* : \underline{u}_c^* : (z_n^*)^2 + 2B : \underline{u}_c : \underline{u}_c^* : |z_n|^2 + \\ &\quad + 2B : \underline{u}_c^* : \underline{\alpha} : z_n |z_n|^2 + 4B : \underline{u}_c : \underline{\beta} : z_n |z_n|^2 \\ &\quad + 3C : \underline{u}_c : \underline{u}_c : \underline{u}_c^* : z_n |z_n|^2 + \dots \end{aligned} \quad (1.33)$$

where here for the last step eq.(1.30) has been used. If we equate contributions of the same order in eqs.(1.32) and (1.33) we obtain the desired coefficients for the normal form (1.31).

Contributions of order $\mathcal{O}(z)$ in eqs.(1.32) and (1.33) match because of the eigenvalue equation (1.29). Matching the contributions of second order, $\mathcal{O}(z^2)$, we obtain, comparing the coefficients of z_n^2 and of $|z_n|^2$

$$\mu_c^2 \underline{\alpha} = \underline{A} \underline{\alpha} + B : \underline{u}_c : \underline{u}_c : \quad (1.34a)$$

$$\underline{\beta} = \underline{A} \underline{\beta} + B : \underline{u}_c : \underline{u}_c^* : \quad (1.34b)$$

The second order contribution associated with $(z_n^*)^2$ just yields the complex conjugate of eq.(1.34a). If $\mu_c \neq 1$ and $\mu_c^2 \neq \mu_c^*$, one can solve eqs.(1.34) since the coefficients appearing on the left hand side are not contained in the spectrum of the matrix \underline{A} . Thus, the parameters of the centre manifold (1.30) are determined by

$$\underline{\alpha} = (\mu_c^2 \underline{1} - \underline{A})^{-1} B : \underline{u}_c : \underline{u}_c : \quad (1.35a)$$

$$\underline{\beta} = (\underline{1} - \underline{A})^{-1} B : \underline{u}_c : \underline{u}_c^* : \quad (1.35b)$$

We now proceed and equate coefficients of the order $\mathcal{O}(\varepsilon z)$ in eqs.(1.32) and (1.33). For the coefficient of εz_n we get

$$\varepsilon \underline{u}_c + \mu_c \underline{\delta} = \underline{\delta} \underline{A} \underline{u}_c + \underline{A} \underline{\delta} \quad (1.36)$$

As μ_c is eigenvalue of the matrix \underline{A} a nontrivial condition, the so called Fredholm condition, has to be imposed on ε in order that eq.(1.36) can be solved for $\underline{\delta}$. In fact, if we multiply eq.(1.36) from the left with the eigenvector \underline{v}_c^\dagger of the adjoint eigenvalue equation (1.29b) the contributions containing $\underline{\delta}$ cancel due to the eigenvalue condition and we are left with

$$\varepsilon \langle \underline{v}_c | \underline{u}_c \rangle = \langle \underline{v}_c | \underline{\delta} \underline{A} \underline{u}_c \rangle \quad (1.37)$$

where we have introduced the usual inner product by $\langle \underline{v} | \underline{u} \rangle = \underline{v}^\dagger \underline{u}$. Eq.(1.37) is nothing else but the well known first order perturbative result for the shift of eigenvalues.

I we finally equate the cubic terms, $z_n |z_n|^2$, in eqs.(1.32) and (1.33) we obtain the condition

$$r \underline{u}_c + \mu_c \underline{\gamma} = 2B : \underline{u}_c^* : \underline{\alpha} : + 4B : \underline{u}_c : \underline{\beta} : + 3C : \underline{u}_c : \underline{u}_c : \underline{u}_c^* : + \underline{A} \underline{\gamma} \quad (1.38)$$

Again application of the Fredholm condition, i.e. multiplication with the adjoint eigenvector, yields the expression for the coefficient of the cubic term

$$r \langle \underline{v}_c | \underline{u}_c \rangle = \langle \underline{v}_c | 2B : \underline{u}_c^* : \underline{\alpha} : + 4B : \underline{u}_c : \underline{\beta} : + 3C : \underline{u}_c : \underline{u}_c : \underline{u}_c^* : \rangle \quad (1.39)$$

Thus all coefficients of the normal form (1.31) have been expressed in terms of quantities of the underlying equation of motion (1.28).

In order to eliminate the other, nonresonant, cubic contributions in the normal form (1.31) which have not been written down explicitly one requires the additional constraints $\mu_c^2 \neq 1$ and $\mu_c^4 \neq 1$ on the critical eigenvalue. When the so called strong resonance conditions, $\mu_c^k = 1$, $k = 1, 2, 3, 4$, are avoided the motion is given in terms of the Hopf normal form⁶.

6 Unlike for differential equations higher-order contribution to the normal form cannot be neglected when the dynamics on the resulting invariant circle is of interest (cf. e.g. [40]).

1.B

Super- and subcritical Hopf bifurcation for maps

Conditions for super- and subcritical behaviour of the time-discrete normal form (1.31) describing the Hopf instability are quite similar to the time-continuous case we dealt with in section 1.3.1. There are, however, minor technical differences and for further reference we just recall the basic facts. A transformation to polar coordinates is in principle possible in the time-discrete setup, but less straightforward. We follow a different strategy and employ a transformation to a rotating frame using $\zeta_n = \mu_c^n z_n$. Then eq.(1.31) reads

$$\zeta_{n+1} - \zeta_n = \frac{\varepsilon}{\mu_c} \zeta_n + \frac{r}{\mu_c} \zeta_n |\zeta_n|^2 . \quad (1.40)$$

In a small neighbourhood of the bifurcation point, i.e. $|\varepsilon| \ll |\mu_c| = 1$, the amplitude $|\zeta_n|$ becomes of order $\mathcal{O}(\sqrt{|\varepsilon|})$ and the rate of change $\zeta_{n+1} - \zeta_n$ turns out to be small as well. Capturing these features with the scaling $\zeta_n = \sqrt{|\varepsilon|} \tilde{\zeta}(|\varepsilon|n)$ one reduces the map (1.40) to the differential equation (1.5) and the conditions of section 1.3.1 on the bifurcation apply. Thus $\text{Re}(\varepsilon/\mu_c) < 0$ yields subthreshold dynamics and $\text{Re}(\varepsilon/\mu_c) > 0$ corresponds to the behaviour beyond the Hopf instability. A supercritical Hopf bifurcation occurs for $\text{Re}(r/\mu_c) < 0$ while $\text{Re}(r/\mu_c) > 0$ yields subcritical behaviour.

Bibliography

- 1 R. Bellmann, *Dynamic programming and modern control theory* (Acad. Press, New York, 1965).
- 2 E. Ott, C. Grebogi, and Y. A. Yorke, *Controlling chaos*, Phys. Rev. Lett. **64**, 1196 (1990).
- 3 T. Shinbrot, *Progress in the control of chaos*, Adv. Phys. **44**, 73 (1995).
- 4 K. Pyragas, *Continuous control of chaos by self-controlling feedback*, Phys. Lett. A **170**, 421 (1992).
- 5 S. Bielawski, D. Derozier, and P. Glorieux, *Controlling unstable periodic orbits by a delayed continuous feedback*, Phys. Rev. E **49**, R971 (1994).
- 6 O. Lüthje, S. Wolff, and G. Pfister, *Control of chaotic Taylor-Couette flow with time-delayed feedback*, Phys. Rev. Lett. **86**, 1745 (2001).
- 7 H. Benner and W. Just, *Control of chaos by time delayed feedback in high power ferromagnetic resonance experiments*, J. Kor. Phys. Soc. **40**, 1046 (2002).
- 8 P. Parmananda, R. Madrigal, M. Rivera, L. Nyikos, I. Z. Kiss, and V. Gáspár, *Stabilization of unstable steady states and periodic orbits in an electrochemical system using delayed-feedback control*, Phys. Rev. E **59**, 5266 (1999).
- 9 T. Hikihara and T. Kawagoshi, *An experimental study on stabilization of unstable periodic motion in magneto-elastic chaos*, Phys. Lett. A **211**, 29 (1996).
- 10 K. Pyragas and A. Tamasevicius, *Experimental control of chaos by delayed self-controlling feedback*, Phys. Lett. A **180**, 99 (1993).
- 11 K. Hall, D. J. Christini, M. Tremblay, J. J. Collins, L. Glass, and J. Billette, *Dynamic control of cardiac alternans*, Phys. Rev. Lett. **78**, 4518 (1997).

- 12 R. Bellmann and K. L. Cooke, *Differential–Difference Equations* (Acad. Press, New York, 1963).
- 13 M. E. Bleich and J. E. S. Socolar, *Controlling spatiotemporal dynamics with time-delayed feedback*, Phys. Rev. E **54**, R17 (1996).
- 14 W. Just, T. Bernard, M. Ostheimer, E. Reibold, and H. Benner, *Mechanism of time-delayed feedback control*, Phys. Rev. Lett. **78**, 203 (1997).
- 15 K. Pyragas, *Analytical properties and optimization of time-delayed feedback control*, Phys. Rev. E **66**, 026207 (2002).
- 16 H. Nakajima, *On analytical properties of delayed feedback control of chaos*, Phys. Lett. A **232**, 207 (1997).
- 17 J. E. S. Socolar, D. W. Sukow, and D. J. Gauthier, *Stabilizing unstable periodic orbits in fast dynamical systems*, Phys. Rev. E **50**, 3245 (1994).
- 18 W. Just, E. Reibold, H. Benner, K. Kacperski, F. Fronczak, and J. Holyst, *Limits of time-delayed feedback control*, Phys. Lett. A **254**, 158 (1999).
- 19 S. Bielawski, D. Derozier, and P. Glorieux, *Experimental characterization of unstable periodic orbits by controlling chaos*, Phys. Rev. A **47**, R2492 (1993).
- 20 H. G. Schuster and M. B. Stemmler, *Control of chaos by oscillating feedback*, Phys. Rev. E **56**, 6410 (1997).
- 21 W. Just, *On the eigenvalue spectrum for time-delayed Floquet problems*, Physica D **142**, 153 (2000).
- 22 K. Pyragas, *Control of chaos via an unstable delayed feedback controller*, Phys. Rev. Lett. **86**, 2265 (2001).
- 23 A. Kittel, J. Parisi, and K. Pyragas, *Delayed feedback control of chaos by self-adapted delay-time*, Phys. Lett. A **198**, 433 (1995).
- 24 H. Nakajima, H. Ito, and Y. Ueda, *Automatic adjustment of delay time and feedback gain in delayed feedback control of chaos*, IE-ICE Trans. Fund. Electr. **E80A**, 1554 (1997).
- 25 W. Just, J. Möckel, D. Reckwerth, E. Reibold, and H. Benner, *Delayed feedback control of periodic orbits in autonomous systems*, Phys. Rev. Lett. **81**, 562 (1998).
- 26 W. Just, D. Reckwerth, E. Reibold, and H. Benner, *Influence of control loop latency on time-delayed feedback control*, Phys. Rev. E **59**, 2826 (1999).
- 27 P. Hövel and J. E. S. Socolar, *Stability domains for time-delay feedback control with latency*, Phys. Rev. E **68**, 036206 (2003).
- 28 *Handbook of Chaos Control*, edited by H. G. Schuster (Wiley–VCH, Berlin, 1999).
- 29 W. Just, H. Benner, and E. Schöll, in *Control of chaos by time-delayed feedback: a survey of theoretical and experimental aspects*, Vol. 43 of *Advances in Solid State Physics*, edited by B. Kramer (Springer, Berlin, 2003), p. 589.
- 30 W. Just, E. Reibold, K. Kacperski, P. Fronczak, J. Holyst, and H. Benner, *Influence of stable Floquet exponents on time-delayed feedback control*, Phys. Rev. E **61**, 5045 (2000).
- 31 O. Beck, A. Amann, E. Schöll, J. E. S. Socolar, and W. Just, *Comparison of time-delayed feedback schemes for spatio-temporal control of chaos in a reaction-diffusion system with global coupling*, Phys. Rev. E **66**, 016213 (2002).
- 32 J. K. Hale and S. M. Verduyn Lunel, *Introduction to Functional Differential Equations* (Springer, New York, 1993).
- 33 K. Engelborghs, T. Luzyanina, and D. Roose, *Numerical bifurcation analysis of delay differential equations*, J. Comp. Appl. Math. **125**, 265 (2000).
- 34 K. Yamasue and T. Hikihara, *Domain of attraction for stabilized orbits in time delayed feedback controlled Duffing systems*, Phys. Rev. E **69**, 056209 (2004).
- 35 C. v. Löwenich, H. Benner, and W. Just, *Experimental relevance of global properties of time-delayed feedback control*, Phys. Rev. Lett. **93**, 174101 (2004).
- 36 W. Just, H. Benner, and C. v. Löwenich, *On global properties of time-delayed feedback control: weakly nonlinear analysis*, Physica D **199**, 33 (2004).
- 37 O. Biham and W. Wenzel, *Characterization of unstable periodic orbits in chaotic attractors and repellers*, Phys. Rev. Lett. **63**, 819 (1989).
- 38 P. Schmelcher and F. K. Diakonou, *Detecting unstable periodic orbits of chaotic dynamical systems*, Phys. Rev. Lett. **78**, 4733 (1997).
- 39 R. L. Davidchack and Y.-C. Lai, *Efficient algorithm for detecting unstable periodic orbits in chaotic systems*, Phys. Rev. E **60**, 6172 (1999).

- 40 J. Guckenheimer and P. Holmes, *Nonlinear Oscillations, Dynamical Systems, and Bifurcations of Vector Fields* (Springer, New York, 1986).
- 41 F. Giannakopoulos and A. Zapp, *Bifurcations in a planar system of differential delay equations modeling neural activity*, *Physica D* **159**, 215 (2001).
- 42 B. F. Redmond, V. G. LeBlanc, and A. Longtin, *Bifurcation analysis of a class of first-order nonlinear delay-differential equations with reflectional symmetry*, *Physica D* **166**, 131 (2002).
- 43 B. Krauskopf and K. Green, *Computing unstable manifolds of periodic orbits in delay differential equations*, *J. Comp. Phys.* **186**, 230 (2003).

Index

- area preserving map, 14
- basin boundary, 8
- basin of attraction, 3, 5, 8, 10, 11, 15
- bifurcation
 - codimension-two, 9, 18
 - continuous, 15
 - discontinuous, 15
 - Hopf, 3, 7, 19
 - local, 7
 - Neimark-Sacker, 7
 - period doubling, 3
 - subcritical, 8, 9, 11, 13, 14, 17, 22
 - supercritical, 8, 11, 13, 14, 17, 22
- Biham-Wenzel method, 5
- bistability, 9
- centre manifold, 19, 21
- control
 - extended TDF, 2
 - latency, 2
 - linear stability, 3, 11, 18
 - non-invasive, 1
 - OGY method, 1
 - Pyragas method, 2
 - rhythmic, 2
- control amplitude, 3
- control performance, 16
- control signal, 3
- control theory, 1
- discontinuous transition, 8
- eigenvalue problem, 11, 19
- Floquet exponent, 3
- hysteresis, 8, 9
- Lyapunov function, 4, 5, 18
- Newton-Raphson method, 5
- normal form, 7, 11, 17, 20
- periodic point, 4
- phase space
 - infinite dimension, 10
- recurrence, 16
- root finding, 4
- strong resonance, 13, 21
- unstable controller, 2